IET Research Journals

Submission Template for IET Research Journal Papers

IET Journals
The Institution of Engineering and Technology

ISSN 1751-8644
doi: 0000000000
www.ietdl.org

Chance-Constrained Maintenance Scheduling for Interdependent Power and Natural Gas Grids Considering Wind Power Uncertainty

Chong Wang[1*], *Zhaoyu Wang*[2], *Jianhui Wang*[3], *Yunhe Hou*[4]

[1] *College of Energy and Electrical Engineering, Hohai University, Nanjing 211100, China*
[2] *Department of Electrical and Computer Engineering, Iowa State University, Ames, IA 50011, USA*
[3] *Department of Electrical Engineering at Southern Methodist University, Dallas, TX 75275, USA*
[4] *Department of Electrical and Electronic Engineering, The University of Hong Kong, Pokfulam, Hong Kong, China*
[*] *E-mail: chongwang@hhu.edu.cn*

Abstract: Considering the increased interactions between power grids and natural gas grids, this paper presents a chance-constrained maintenance scheduling model for integrated gas-electric grids with wind energy integration. Given the uncertainties of wind power, the loss of wind power probability is modeled as a chance constraint, ensuring the high utilization of wind power. To overcome the adversities caused by the nonlinear and non-convex models of natural gas systems, a piecewise linear approximation method is employed to transform the nonlinear models into a group of mixed integer linear models. A big-M formulation method is used to construct inequalities constraints for lines/pipelines to be under maintenance. In addition, unit commitment is also coordinated to achieve the best maintenance strategies. The proposed chance-constrained stochastic programming model is converted into an equivalent deterministic programming model via a strong extended formulation for the sample average approximation by leveraging the star-inequalities. Several tests on a 4-node natural gas system with a 6-bus power system and a 20-node natural gas system with a modified IEEE 118-bus power system demonstrate the effectiveness of the proposed model.

Nomenclature

Indices and Sets

w	Index of wind farms.
g	Index of generators.
$\bar{g}$	Index of gas wells.
$\tilde{g}$	Index of gas storages.
b, b'	Index of power buses.
n, n'	Index of natural gas nodes.
l'	Index of lines that need not to be under maintenance within the given time window.
l	Index of lines that need to be under maintenance within the given time window.
p'	Index of pipelines that need not to be under maintenance within the given time window.
p	Index of pipelines that need to be under maintenance within the given time window.
$\bar{p}$	Index of pipelines with compressors.
s	Index of wind power generation scenarios.
t, t'	Index of time periods.
k	Index of piecewise segments for gas flow.
$\mathcal{L}$	Set of lines that need to be under maintenance within the given time window.
$\mathcal{P}$	Set of pipelines that need to be under maintenance within the given time window.
$\mathcal{T}$	Set of time periods.
$\mathcal{W}$	Set of wind farms.
$\mathcal{S}$	Set of wind power generation scenarios.
$\mathcal{G}$	Set of generators.
$\mathcal{G}_b$	Set of generators connected to power bus b.
$\mathcal{W}_b$	Set of wind farms connected to power bus b.
$\mathcal{N}_n$	Set of gas nodes connected to gas node n.
$\mathcal{N}$	Set of gas nodes.
$\tilde{\mathcal{G}}_n$	Set of gas storages connected to gas node n.
$\bar{\mathcal{G}}_n$	Set of gas wells connected to gas node n.
$\mathcal{G}_n$	Set of gas-fired units connected to gas node n.
$\mathcal{B}_b$	Set of power buses connected to power bus b.
$\mathcal{B}$	Set of power buses.

Parameters

$A^k_{p,t}, A^k_{p',t}$	Slopes of piecewise linear segments.
$B^k_{p,t}, B^k_{p',t}$	Intercept of piecewise linear segments.
$B_{b,b'}$	Electrical susceptance of line $b-b'$.
$C^M_{l,t}, C^M_{p,t}$	Maintenance costs of line l and pipeline p at t.
$C^F_{g,t}, C^L_{g,t}$	Fixed cost and revenue of generator g at t.
$C^S_{g,t}$	Start-up cost of generator g at t.
$C_{\bar{g},t}, C_{\tilde{g},t}$	Revenues of gas well $\bar{g}$ and storage $\tilde{g}$ at t.
$C^{LS}_{b,t}, C^{LS}_{n,t}$	Penalty costs of power/gas load shedding at t.
$C_{n,n'}$	Weymouth constant of pipeline $n-n'$.
D^{on}_g, D^{off}_g	Minimum on and off time periods of generator g.
$D^{on}_{\bar{g}}, D^{off}_{\bar{g}}$	Minimum on and off time periods of gas well $\bar{g}$.
D^M_l, D^M_p	Duration of maintenance of line l and pipeline p.
EF_g	Efficiency factor of gas-fired unit g.
$\underline{f}^k_p, \underline{f}^k_{p'}$	Lower limits of gas flow through piecewise segments.

$\underline{f}_p^k, \overline{f}_{p'}^k$	Upper limits of gas flow through piecewise segments.
$\underline{G}_{\bar{g}}, \overline{G}_{\bar{g}}$	Lower and upper outputs of gas well $\bar{g}$.
$\underline{S}_{\tilde{g}}, \overline{S}_{\tilde{g}}$	Lower and upper outputs of gas storage $\tilde{g}$.
M	A large number.
$L_{b,t}, L_{n,t}$	Power load of bus b at t and gas load of node n at t.
N_t^{LM}	Maximum number of lines that can be under maintenance at t.
N_t^{PM}	Maximum number of pipelines that can be under maintenance at t.
$\underline{P}_g, \overline{P}_g$	Lower and upper limits of generator g.
$\underline{P}_{b,b'}^L, \overline{P}_{b,b'}^L$	Lower and upper capacities of line $b-b'$.
P_w^{max}	Maximum capacity limit of wind generator w.
$\tilde{P}_{w,t}$	Random number representing the available wind energy generated from wind generator w at t.
$\tilde{P}_{w,t,s}$	sth sample of wind power realization for wind generator w at t.
$\underline{R}_g, \overline{R}_g$	Ramp-up and ramp-down limits of generator g.
$\underline{R}_{\tilde{g}}, \overline{R}_{\tilde{g}}$	In-flow and out-flow limits of gas storage $\tilde{g}$.
$\underline{\theta}_b, \overline{\theta}_b$	Lower/upper limits of phase angles at bus b.
$\overline{\theta}_{b,b'}$	Phase angle difference limit of line $b-b'$.
$\underline{\pi}_n, \overline{\pi}_n$	Minimum/maximum squared pressures.
$\lambda_{\bar{p}}$	Compression factor.
ϵ	Risk level of the chance constraint.
α	Percent of wind energy utilized.
Variables	
υ_s	Binary variable with regard to SAA.
$\beta_{w,t}$	Continuous variable for strong extended formulation of SAA.
$r_i, \gamma_{w,t,i}$	Binary variables for strong extended formulation of SAA.
$\Delta L_{b,t}$	Power load shedding of bus b at t.
$\Delta L_{n,t}$	Gas load shedding of gas node n at t.
$L_{g,t}$	Gas consumption of gas-fired unit g at t.
$S_{\tilde{g},t}, S_{\tilde{g},t-1}$	Gas inventory of gas storage $\tilde{g}$ at t and $t-1$.
$G_{\bar{g},t}$	Gas production of gas well $\bar{g}$ at t.
$f_{p',t}^k, f_{p,t}^k$	Piecewise linear gas flow at t.
$F_{n,n'}$	Gas flow from gas node n to gas node n' at t.
$m_{p,t}$	Binary variables indicating whether pipeline p is under maintenance at t. '0' means maintenance, otherwise '1'.
$m_{l,t}$	Binary variables indicating whether line l is under maintenance at t. '0' means maintenance, otherwise '1'.
$PS_{n,t}$	Pressure of gas node n at t.
$P_{b,b',t}^L$	Power from bus b to bus b' at t.
$P_{g,t}$	Power generation of generator g at t.
$P_{w,t}$	Power generated by wind generator w at t.
$o_{\bar{g},t}$	Binary variables indicating the state of gas well $\bar{g}$ at t. '0' and '1' denote off and on states, respectively.
$o_{g,t}$	Binary variables indicating the state of generator g at t. '0' and '1' denote off and on states, respectively.
$u_{g,t}$	Binary variable indicating whether generator g is started up at t.
$\pi_{n,t}, \pi_{n',t}$	Squared pressures of gas nodes n and n' at t.
$\theta_{b,t}, \theta_{b',t}$	Phase angles of bus b and bus b' at t.
$\eta_{p',t}^k, \eta_{p,t}^k$	Binary variables to indicating whether the piecewise linear function k is selected. '0' denotes 'non-selected', and '1' denotes 'selected'.

1 Introduction

To use more green electricity, more natural gas-fired units are deployed in power systems. According to the data from the Energy Information Administration, natural gas supplied 32.1% of total U.S. electricity at utility-scale power plants in the first quarter of 2016 [1], and over 60% of new generation will be fueled by natural gas from 2025 to 2040 in the U.S.[2]. Increasing natural gas-fired units make power systems and natural gas systems have stronger couple. An outage or an interruption in natural gas grids could cause the loss of gas supply to gas-fired units, and in consequence could jeopardize the power system security and further lead to power load shedding [3]. For example, a failure on a single pipeline in 2002 resulted in the loss of 2019 MW power generation in Chicago, and further caused a cascading power outage. More than 10000 failures in gas pipeline networks, resulting in six billion U.S. dollars of damages and losses in natural gas systems and power systems, were reported by the Pipeline and Hazardous Materials Safety Administration (2013) of U.S. Department of Transportation. In this case, it is essential to guarantee high reliability of the interdependent power grids and natural gas grids. Usually, maintenance is used as one of important means to maintain high component reliability [4]. In addition, the percentage of wind power in power systems continues to increase, led by Uruguay, Portugal and Ireland pushing over 20%, followed by Spain around 20%, Germany around 16%. The big markets of Canada, U.S. and China get 6%, 5.5% and 4% of their electricity power from wind, respectively [5]. Based on the report of U.S. Department of Energy, 20% of electricity in U.S. will be generated by wind by 2030 [6], and more than 6.5% of world electricity will be generated from wind [7]. Though wind power can help to reduce the emissions of electricity production, high inter-temporal variations of wind power and its weak predictability also cause a series of new challenges to power system operation. Considering the requirement of high reliability of gas-power grids and the increasing integration of wind power into power grids, it is imperative to coordinate maintenance on interdependent natural gas and power grids with increasing wind power.

There have been some studies on integrated gas and power grid. In [8], a two-stage expansion planning model, in which uncertainty caused by natural gas and electricity demands is included, is developed. In [10], a framework for designing interdependent natural gas and electricity networks is presented, by which the types and the capacities of the components can be determined. Considering dynamic gas flows on pipeline grids, a day-ahead scheduling model is proposed in [11] for generating unit dispatch and natural gas compressor operation. A decentralized optimal energy flow calculation method is developed in [12] to deal with possible multiple subsystems that are tied by means of natural gas and power grids. In [13], an approximated transient matrix-form gas flow model is developed to include the influences of dynamics of natural gas flow on power systems. [14] investigates reverse power flow for distribution systems in consideration of integrated natural gas systems under renewable power penetration. [15] analyzes the potential of power-to-gas grids in consideration of the characteristics and the constraints of natural gas and power grids. [16] investigates the equilibrium of the coupled electricity and natural gas markets in consideration of market clearing processes. [17] proposes a two-stage mixed-integer linear stochastic optimization model to analyze the scheduling of electricity production units under natural gas-supply uncertainty due to pipeline congestion and natural gas-price variability. [18] proposes a long-term robust co-optimization planning model for Interdependent Electricity and Natural Gas Systems to minimize the total investment and operation costs. To deal with increasing extreme events,

[19] proposes a preventive strategy for integrated natural gas and power systems to enhance the power system resilience. [20] proposes a graph-based framework, which facilitates analysis and simulation application for coupled infrastructure networks. However, no research studies focus on coordinated maintenance on interdependent natural gas and power grids, especially when including wind power.

Due to variability and uncertainty, a large amount of reserve capacity is required to accommodate forecast errors of wind power. When reserve capacity is not enough or transmission congestion exists, power system operators need to curtail wind power to guarantee the safty of the system. Robust optimization [21] can be used to deal with variability and uncertainty in consideration of operating conditions, however, it is based on the worst case outcomes that will lead to a too conservative results. In practice, system operators desire to utilize wind power as much as possible, and to be able to request a portion of wind power at a certain probability. Chance-based constraints can be used to deal with the above issue and to describe the percentage of utilized wind power [22–26].

Therefore, we use chance-constrained model to formulate the problem of scheduling maintenance for integrated natural gas grids and power grids in consideration of wind power. The main contributions of this paper are shown as follows: 1) A model for maintenance scheduling for integrated natural gas and power grids with uncertain wind power is constructed; 2) Chance constraints are used to describe the utilization of wind power, and they are converted into a group of mixed integer liner constraints by means of a strong extended formulation for the sample average approximation based on the star-inequalities; 3) A big-M formulation method is used to construct inequalities constraints for pipelines/lines that need to be under maintenance within the given time window; 4) The influences of natural gas grids on system maintenance scheduling are analyzed.

The remainder of this paper is organized as follows. The maintenance scheduling formulation, including the optimization objective, the maintenance constraints, the operating constraints of power and natural gas grids, are shown in Section 2. Section 3 presents the strong extended formulation of sample average approximation, and Section 4 presents the case studies. The work is concluded in Section 5.

2 Maintenance Scheduling Formulation

2.1 Optimization Objective

The objective is to maximize the revenue of the natural gas and power grid under maintenance. The detailed objective can be expressed as follows.

$$\begin{aligned}\max \quad & \underbrace{\sum_{g\in\mathcal{G}}\sum_{t\in\mathcal{T}}(C^L_{g,t}\cdot P_{g,t}-C^F_{g,t}\cdot o_{g,t}-C^S_{g,t}\cdot u_{g,t})}_{(1a)}+\\ & \underbrace{\sum_{\tilde{g}\in\tilde{\mathcal{G}}}\sum_{t\in\mathcal{T}}(C_{\tilde{g},t}\cdot G_{\tilde{g},t})}_{(1b)}+\underbrace{\sum_{\tilde{g}\in\tilde{\mathcal{G}}}\sum_{t\in\mathcal{T}}(C_{\tilde{g},t}\cdot S_{\tilde{g},t})}_{(1c)}-\\ & \underbrace{\sum_{l\in\mathcal{L}}\sum_{t\in\mathcal{T}}(C^M_{l,t}\cdot(1-m_{l,t}))}_{(1d)}-\underbrace{\sum_{p\in\mathcal{P}}\sum_{t\in\mathcal{T}}(C^M_{p,t}\cdot(1-m_{p,t}))}_{(1e)}-\\ & \underbrace{\sum_{b\in\mathcal{B}}\sum_{t\in\mathcal{T}}(C^{LS}_{b,t}\cdot\Delta L_{b,t})}_{(1f)}-\underbrace{\sum_{n\in\mathcal{N}}\sum_{t\in\mathcal{T}}(C^{LS}_{n,t}\cdot\Delta L_{n,t})}_{(1g)}\end{aligned} \tag{1}$$

where (1a) is the revenue from the power grid, (1b) and (1c) are the revenues from the natural gas system, (1d) and (1e) present the costs of maintenance on lines and pipelines, respectively. (1f) and (1g) are the costs of penalties caused by non-served power load and gas load, respectively.

2.2 Constraints of Maintenance

When performing maintenance, some constraints of maintenance should be satisfied.

$$\begin{aligned}&m_{l,t-1}-m_{l,t}+m_{l,t'}\le 1\\ &1\le t'-(t-1)\le D^M_l,\forall t,l\end{aligned} \tag{2}$$

$$\begin{aligned}&m_{p,t-1}-m_{p,t}+m_{p,t'}\le 1\\ &1\le t'-(t-1)\le D^M_p,\forall t,p\end{aligned} \tag{3}$$

$$\sum_{t\in\mathcal{T}}(1-m_{l,t})=D^M_l\quad\forall l \tag{4}$$

$$\sum_{t\in\mathcal{T}}(1-m_{p,t})=D^M_p\quad\forall p \tag{5}$$

$$\sum_{l\in\mathcal{L}}(1-m_{l,t})\le N^{LM}_t\quad\forall t \tag{6}$$

$$\sum_{p\in\mathcal{P}}(1-m_{p,t})\le N^{PM}_t\quad\forall t \tag{7}$$

where (2) and (3) ensure the minimal durations of maintenance activities on lines and pipelines, respectively. (4) and (5) ensure that maintenance activities on lines and pipelines will be implemented during the given time window. (6) shows the maximum number of lines that can be under maintenance within one time period, and (7) shows the similar constraint for pipelines.

2.3 Operation Constraints of Power Grids

For a power gird, the operation constraints, e.g., power balance, ramping rates of generators, generation limits and voltage limits, should be satisfied. The detailed constraints are listed as follows.

$$\Pr\left\{\begin{array}{l}\sum_{w\in\mathcal{W}}\sum_{t\in\mathcal{T}}P_{w,t}\ge\alpha\sum_{w\in\mathcal{W}}\sum_{t\in\mathcal{T}}\tilde{P}_{w,t},\\ P_{w,t}\le\tilde{P}_{w,t}\quad\forall w,t\end{array}\right\}\ge 1-\epsilon \tag{8}$$

$$\begin{aligned}&\sum_{g\in\mathcal{G}_b}P_{g,t}+\sum_{w\in\mathcal{W}_b}P_{w,t}-\left(L_{b,t}-\Delta L_{b,t}\right)\\ &\qquad+\sum_{b'\in\mathcal{B}_b}P^L_{b,b',t}=0\qquad\forall t,b\end{aligned} \tag{9}$$

$$\begin{aligned}&B_{b,b'}\cdot\left(\theta_{b,t}-\theta_{b',t}\right)-P^L_{b,b',t}+(1-m_{l,t})\cdot M\ge 0\\ &\qquad\forall t,l,(b,b')\in l\end{aligned} \tag{10}$$

$$\begin{aligned}&B_{b,b'}\cdot\left(\theta_{b,t}-\theta_{b',t}\right)-P^L_{b,b',t}-(1-m_{l,t})\cdot M\le 0\\ &\qquad\forall t,l,(b,b')\in l\end{aligned} \tag{11}$$

$$\underline{P}^L_{b,b'}\cdot m_{l,t}\le P^L_{b,b',t}\le\overline{P}^L_{b,b'}\cdot m_{l,t}\qquad\forall t,(b,b')\in l,l \tag{12}$$

$$B_{b,b'}\cdot\left(\theta_{b,t}-\theta_{b',t}\right)=P^L_{b,b',t}\qquad\forall t,l',(b,b')\in l' \tag{13}$$

$$\underline{P}^L_{b,b'}\le P^L_{b,b',t}\le\overline{P}^L_{b,b'}\qquad\forall t,(b,b')\in l',l' \tag{14}$$

$$\begin{aligned}&-o_{g,t-1}+o_{g,t}-o_{g,t'}\le 0\\ &1\le t'-(t-1)\le D^{ON}_g,\forall g,t\end{aligned} \tag{15}$$

$$\begin{aligned}&o_{g,t-1}-o_{g,t}+o_{g,t'}\le 1\\ &1\le t'-(t-1)\le D^{OFF}_g,\forall g,t\end{aligned} \tag{16}$$

$$-o_{g,t-1}+o_{g,t}-u_{g,t}\le 0\qquad\forall g,t \tag{17}$$

$$\underline{P}_g\cdot o_{g,t}\le P_{g,t}\le\overline{P}_g\cdot o_{g,t}\qquad\forall g,t \tag{18}$$

$$\begin{aligned}&\left|\theta_{b,t}-\theta_{b',t}\right|\le m_{l,t}\cdot\bar{\theta}_{b,b'}+(1-m_{l,t})\cdot M\\ &\qquad\forall t,(b,b')\in l,l\end{aligned} \tag{19}$$

$$\left|\theta_{b,t}-\theta_{b',t}\right| \le \overline{\theta}_{b,b'} \quad \forall t,(b,b') \in l',l' \tag{20}$$

$$0 \le \Delta L_{b,t} \le L_{b,t} \qquad \forall t,b \tag{21}$$

$$\begin{aligned} P_{g,t}-P_{g,t-1} \le (2-o_{g,t-1}-o_{g,t})\cdot \underline{P}_g + \\ +(1+o_{g,t-1}-o_{g,t})\cdot \overline{R}_g \qquad \forall g,t \end{aligned} \tag{22}$$

$$\begin{aligned} P_{g,t-1}-P_{g,t} \le (2-o_{g,t-1}-o_{g,t})\cdot \underline{P}_g + \\ +(1-o_{g,t-1}+o_{g,t})\cdot \underline{R}_g \qquad \forall g,t \end{aligned} \tag{23}$$

$$P_{g,t} = L_{g,t}\cdot EF_g \quad \forall g \in \mathcal{G}_n, t \tag{24}$$

where (8) shows the chance constraint ensuring that the scheduled wind power is within a certain range with a probability of $1-\epsilon$, and Pr denotes the probability. $\sum_{w\in\mathcal{W}}\sum_{t\in\mathcal{T}} P_{w,t} \ge \alpha \sum_{w\in\mathcal{W}}\sum_{t\in\mathcal{T}} \tilde{P}_{w,t}$ represents that α percent of available wind power can be dispatched. $P_{w,t} \le \tilde{P}_{w,t}$ shows that the scheduled wind power is not beyond the available wind power. (9) enforces power balance at each node in each time interval. (10) and (11) represent the physical relations between voltage angles and power flows in transmission lines to be under maintenance. M is a disjunctive constant. (10) and (11) are redundant when the corresponding lines are under maintenance with a sufficiently large M. (12) ensures the lower and upper bounds for power flows through lines to be under maintenance. (13) relates the voltage angles and power flows through the lines that need not to be under maintenance, and (14) shows the lower/upper limits of power flow through the corresponding lines. (15) and (16) denote the minimum on-time and off-time of the generator g. (17) represents the start-up constraint of the generator g. (18) is the capacity limit of the generator g. The constraint (19) shows the limit of the phase angle difference of the line that needs to be under maintenance, and (20) shows the limit of the phase angle difference of the line that needs not be to under maintenance, (21) enforces the limits of load shedding. (22) and (23) present the ramp-up/ramp-down constraints of generators. (24) shows the relation between real power from gas-fired units and natural gas consumption .

2.4 *Operation Constraints of Natural Gas Systems*

The critical components in a natural gas (NG) gird include gas wells, gas storages, pipelines, compressors, and gas loads. For these components, we consider the following operation constraints.

2.4.1 NG production: Gas production of each gas well is limited by its minimum and maximum values.

$$\underline{G}_{\bar{g}}\cdot o_{\bar{g},t} \le G_{\bar{g},t} \le \overline{G}_{\bar{g}}\cdot o_{\bar{g},t} \qquad \forall \bar{g},t \tag{25}$$

$$\begin{aligned} -o_{\bar{g},t-1}+o_{\bar{g},t}-o_{\bar{g},t'} \le 0 \\ 1 \le t'-(t-1) \le D^{on}_{\bar{g}}, \forall \bar{g},t \end{aligned} \tag{26}$$

$$\begin{aligned} o_{\bar{g},t-1}-o_{\bar{g},t}+o_{\bar{g},t'} \le 1 \\ 1 \le t'-(t-1) \le D^{off}_{\bar{g}}, \forall \bar{g},t \end{aligned} \tag{27}$$

where (25) is the lower/upper limit of the gas well $\bar{g}$ at t, and (26) and (27) denote the minimum on-time and off-time constraints of the gas well $\bar{g}$.

2.4.2 NG storages: The maximum storage level should be within the constraints.

$$\underline{S}_{\tilde{g}} \le S_{\tilde{g},t} \le \overline{S}_{\tilde{g}} \qquad \forall \tilde{g},t \tag{28}$$

$$\underline{R}_{\tilde{g}} \le S_{\tilde{g},t}-S_{\tilde{g},t+1} \le \overline{R}_{\tilde{g}} \quad \forall \tilde{g},t \tag{29}$$

where (28) is the lower/upper limit of the gas storage, and (29) shows the limit of out-flow and in-flow rates of the storage.

2.4.3 Natural gas balance: Natural gas balance at each gas node should be ensured in each time period.

$$\begin{aligned} \sum_{\bar{g}\in\bar{\mathcal{G}}_n} G_{\bar{g},t} + \sum_{\tilde{g}\in\tilde{\mathcal{G}}_n}\left(S_{\tilde{g},t-1}-S_{\tilde{g},t}\right) - \sum_{n'\in\mathcal{N}_n} F_{n,n',t} \\ - \sum_{g\in\mathcal{G}_n}\left(L_{g,t}\cdot EF_g\right) - \left(L_{n,t}-\Delta L_{n,t}\right) = 0 \quad \forall n,t \end{aligned} \tag{30}$$

$$0 \le \Delta L_{n,t} \le L_{n,t} \qquad \forall t,n \tag{31}$$

where (30) denotes the gas balance of the gas node n in each time interval, and (31) shows the limit of gas load shedding.

2.4.4 NG flow in pipelines not to be under maintenance: The pressure drops in pipelines can be expressed as the nonlinear Weymouth (8).

$$\text{sign}(F_{n,n',t})\cdot F^2_{n,n',t} = C^2_{n,n'}\cdot\left(PS^2_{n,t}-PS^2_{n',t}\right) \quad \forall n,n',t \tag{32}$$

However, (32) leads to difficulty in solving the model. In this paper, a piecewise linear approach, as shown in Fig. 1, is employed by using the mixed integer programming. After substituting PS^2 with π, the left side of (32) can be written as the sum of a series of linear functions approximately.

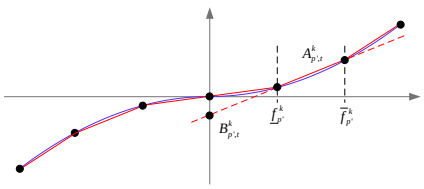

Fig. 1: Piecewise linear approximation of pipeline flow.

The model can be expressed as (**??**) for the pipelines that need not to be under maintenance within the given time window.

$$\begin{aligned} \sum_k \left(A^k_{p',t}\cdot f^k_{p',t} + B^k_{p',t}\cdot \eta^k_{p',t}\right) \\ = C^2_{n,n'}\left(\pi_{n,t}-\pi_{n',t}\right) \quad \forall t,\ (n,n') \in p',p' \end{aligned} \tag{33}$$

$$\sum_k \eta^k_{p',t} = 1 \quad \forall p',t \tag{34}$$

$$\eta^k_{p',t}\cdot \underline{f}^k_{p'} \le f^k_{p',t} \le \eta^k_{p',t}\cdot \overline{f}^k_{p'} \quad \forall k,t,p' \tag{35}$$

$$F_{n,n',t} = \sum_k f^k_{p',t} \quad \forall\ (n,n') \in p',t,p' \tag{36}$$

$$\eta^k_{p',t} \in \{0,1\} \quad \forall p',k,t \tag{37}$$

where the term $F_{n,n',t}\cdot\left|F_{n,n',t}\right|$ in (32) is approximated by the sum of piecewise linear functions on the left side of (33). For example, six piecewise linear functions, i.e., $k=\{1,2,\cdots,6\}$, exist in Fig. 1. (34) guarantees that only one function can be selected with the constraint $\eta^k_{p',t} \in \{0,1\}$. For the kth linear function, the variable $f^k_{p',t}$ is limited by (35). (36) shows the gas flow through the pipeline $n-n'$.

2.4.5 NG flow in pipelines to be under maintenance: A piecewise linear approximation approach with a big-M approach is

employed to model the pipelines that need to be under maintenance.

$$\sum_k \left(A^k_{p,t} \cdot f^k_{p,t} + B^k_{p,t} \cdot \eta^k_{p,t}\right) \le C^2_{n,n'} \left(\pi_{n,t} - \pi_{n',t}\right) + (1 - m_{p,t}) \cdot M \quad \forall (n,n') \in p,t,p \tag{38}$$

$$\sum_k \left(A^k_{p,t} \cdot f^k_{p,t} + B^k_{p,t} \cdot \eta^k_{p,t}\right) \ge C^2_{n,n'} \left(\pi_{n,t} - \pi_{n',t}\right) - (1 - m_{p,t}) \cdot M \quad \forall (n,n') \in p,t,p \tag{39}$$

$$\eta^k_{p,t} \cdot \underline{f}^k_p \le f^k_{p,t} \le \eta^k_{p,t} \cdot \overline{f}^k_p \quad \forall p,k,t \tag{40}$$

$$F_{n,n',t} = \sum_k f^k_{p,t} \quad \forall (n,n') \in p,t,p \tag{41}$$

$$\sum_k \eta^k_{p,t} = m_{p,t} \quad \forall p,t \tag{42}$$

$$m_{p,t}, \eta^k_{p,t} \in \{0,1\} \quad \forall k,t,p \tag{43}$$

where gas flows through pipelines are represented as (38) and (39). When the pipelines are under maintenance, (38) and (39) are redundant by introducing a sufficiently large M and a binary variable $m_{p,t}$. (40) and (41) present the similar meanings with (35) and (36), respectively. (42) shows the relation between the variable $\eta^k_{p,t}$ and $m_{p,t}$. When $m_{p,t} = 1$, the corresponding pipeline is not under maintenance and the corresponding models are the same as (33)-(36). When $m_{p,t} = 0$, the corresponding pipeline is under maintenance, and the corresponding constraints are redundant.

2.4.6 NG pressure constraints: In natural gas grids, the pressure of each node needs to be within the limit.

$$\underline{\pi}_n \le \pi_{n,t} \le \overline{\pi}_n \quad \forall n,t \tag{44}$$

$$\pi_{n',t} \le \lambda_{\bar{p}} \cdot \pi_{n,t} \quad \forall \bar{p},t,(n,n') \in \bar{p} \tag{45}$$

where (44) shows the pressure constraint. For a pipeline with a compressor, the pressures between the out-coming gas node and the in-coming gas node should satisfy the constraint (45).

3 Strong Extended Formulation of Sample Average Approximation

This section first introduces the conventional sample average approximation, and then a strong extended formulation of the sample average approximation is presented.

3.1 Conventional Sample Average Approximation

Let $\tilde{P}_{w,t,s}, w \in \mathcal{W}, t \in \mathcal{T}, m \in \mathcal{S}$ be independent Monte Carlo samples of the random parameter $\tilde{P}_{w,t}$ in (8). With $\tilde{P}_{w,t,s}$, we can build the following formulation (46)-(49) to replace the chance constraint (8) by using the Sample Average Approximation (SAA) approach.

$$\sum_{w\in\mathcal{W}} \sum_{t\in\mathcal{T}} P_{w,t} + \upsilon_s M \ge \alpha \sum_{w\in\mathcal{W}} \sum_{t\in\mathcal{T}} \tilde{P}_{w,t,s} \quad \forall s \tag{46}$$

$$P_{w,t} - \upsilon_s M \le \tilde{P}_{w,t,s} \quad \forall w,t,s \tag{47}$$

$$\sum_{s\in\mathcal{S}} \upsilon_s \le \epsilon \left|\mathcal{S}\right| \tag{48}$$

$$\upsilon_s \in \{0,1\} \quad \forall s \tag{49}$$

where $|\mathcal{S}|$ denotes the number of samples, and M is a large positive constant. υ_s is a binary variable, representing if the sth scenario is satisfied or not. When $\upsilon_s = 0$, the constraints $\sum_{w\in\mathcal{W}} \sum_{t\in\mathcal{T}} P_{w,t} \ge \alpha \sum_{w\in\mathcal{W}} \sum_{t\in\mathcal{T}} \tilde{P}_{w,t,s}$ and $P_{w,t} \le \tilde{P}_{w,t,s}$ holds. When $\upsilon_s = 1$, the constraints with respect to the sth scenario become redundant. The constraint (48) shows that the number of scenarios that violate the chance constraint does not exceed $\epsilon |\mathcal{S}|$. In this way, the original chance constraint is approximated by counting the number of scenarios that satisfy some deterministic constraints.

3.2 Strong Extended Formulation of SAA

With the conventional SAA, the size of the formulation grows rapidly as the number of samples increases. To deal with this issue, a strong extended formulation of SAA is employed. We first rewrite the formulation (46)-(49).

$$\sum_{w\in\mathcal{W}} \sum_{t\in\mathcal{T}} P_{w,t} + \upsilon_s(\alpha \sum_{w\in\mathcal{W}} \sum_{t\in\mathcal{T}} \tilde{P}_{w,t,s}) \ge \alpha \sum_{w\in\mathcal{W}} \sum_{t\in\mathcal{T}} \tilde{P}_{w,t,s} \quad \forall s \tag{50}$$

$$\beta_{w,t} + \upsilon_s(P^{\max}_w - \tilde{P}_{w,t,s}) \ge P^{\max}_w - \tilde{P}_{w,t,s} \quad \forall w,t,s \tag{51}$$

$$\beta_{w,t} = P^{\max}_w - P_{w,t} \quad \forall w,t \tag{52}$$

$$\sum_{s\in\mathcal{S}} \upsilon_s \le \epsilon \left|\mathcal{S}\right| \tag{53}$$

$$\upsilon_s \in \{0,1\} \quad \forall s \tag{54}$$

where (46) is converted to (50), and (47) is converted to (51) and (52). Take the constraint (46) as an example. There are two scenarios: when $\upsilon_s = 0$, $\sum_{w\in\mathcal{W}} \sum_{t\in\mathcal{T}} P_{w,t} \ge \alpha \sum_{w\in\mathcal{W}} \sum_{t\in\mathcal{T}} \tilde{P}_{w,t,s} \quad \forall s$ holds; when $\upsilon_s = 1$, $\sum_{w\in\mathcal{W}} \sum_{t\in\mathcal{T}} P_{w,t} + M \ge \alpha \sum_{w\in\mathcal{W}} \sum_{t\in\mathcal{T}} \tilde{P}_{w,t,m} \quad \forall s$ holds. For the new constraint (50), when $\upsilon_s = 0$, $\sum_{w\in\mathcal{W}} \sum_{t\in\mathcal{T}} P_{w,t} \ge \alpha \sum_{w\in\mathcal{W}} \sum_{t\in\mathcal{T}} \tilde{P}_{w,t,s} \quad \forall s$ holds; when $\upsilon_s = 1$, $\sum_{w\in\mathcal{W}} \sum_{t\in\mathcal{T}} P_{w,t} + \alpha \sum_{w\in\mathcal{W}} \sum_{t\in\mathcal{T}} \tilde{P}_{w,t,s} \ge \alpha \sum_{w\in\mathcal{W}} \sum_{t\in\mathcal{T}} \tilde{P}_{w,t,s} \quad \forall s$ holds since $P_{w,t} \ge 0$. This shows that (50) is sufficient for (46).

For the formulation (50)-(51), the star-inequalities can be used to build the strong extended formulation [27]. To this end, we first sort $\alpha \sum \sum_{w\in W,t\in T} \tilde{P}_{w,t,s}$ and $P^{\max}_w - \tilde{P}_{w,t,s}$ in descending order and define the index of the element at the i^{th} position of the sequence as $s(i)$ where $i \in \mathcal{I}$ and $\mathcal{I} = \{1,2,\cdots \lfloor \epsilon |\mathcal{S}| \rfloor\}$. $\lfloor \epsilon |\mathcal{S}| \rfloor$ denotes the largest integer but less than $\epsilon |\mathcal{S}|$. By introducing new binary variables r_i and $\gamma_{w,t,i}$, the strong extended formulation can be rewritten as follows.

$$\sum_{w\in\mathcal{W}} \sum_{t\in\mathcal{T}} P_{w,t} + \alpha \sum_{i\in\mathcal{I}} \left(r_i \cdot \sum_{w\in\mathcal{W}} \sum_{t\in\mathcal{T}} \tilde{P}_{w,t,s(i)} - r_i \cdot \sum_{w\in\mathcal{W}} \sum_{t\in\mathcal{T}} \tilde{P}_{w,t,s(i+1)} \right) \ge \alpha \sum_{w\in\mathcal{W}} \sum_{t\in\mathcal{T}} \tilde{P}_{w,t,s(1)} \tag{55}$$

$$r_i - r_{i+1} \ge 0 \quad \forall i \tag{56}$$

$$\upsilon_{s(i)} - r_i \ge 0 \quad \forall i \tag{57}$$

$$\beta_{w,t} + \sum_{i\in\mathcal{I}} \left((\tilde{P}_{w,t,s(i+1)} - \tilde{P}_{w,t,s(i)}) \cdot \gamma_{w,t,i} \right) \ge P^{\max}_w - \tilde{P}_{w,t,s(1)} \quad \forall w,t \tag{58}$$

$$\gamma_{w,t,i} - \gamma_{w,t,i+1} \geq 0 \quad \forall i, w, t \tag{59}$$

$$\upsilon_{s(i)} - \gamma_{w,t,i} \geq 0 \quad \forall i, w, t \tag{60}$$

$$\beta_{w,t} = P_w^{\max} - P_{w,t} \quad \forall w, t \tag{61}$$

$$\sum_{s \in \mathcal{S}} \upsilon_s \leq \epsilon |\mathcal{S}| \tag{62}$$

$$\upsilon_s, \gamma_{w,t,i}, r_i \in \{0, 1\} \quad \forall s, w, t, i \tag{63}$$

3.3 Reformulated Optimization Model

The reformulated optimization model can be rewritten as follows.

$$\begin{aligned} Obj. \quad & (1) \\ s.t. \quad & (2) - (7) \\ & (9) - (24) \\ & (25) - (45) \\ & (55) - (63) \end{aligned}$$

where the reformulated optimization model is a mixed integer linear programming model, which is solved by the solver CPLEX.

4 Case Studies

The proposed model is verified by two test systems. The first one is a 4-node natural gas grid with a 6-bus power grid, and the second one is a 20-node natural gas grid with a modified IEEE 118-bus power grid.

4.1 4-node natural gas grid with 6-bus power grid

4.1.1 Test system description: The 4-node natural gas grid and the 6-bus power grid are detailed in [28] and [29]. The integrated systems are shown in Fig. 2. The trend of wind power generation is the Belgian wind-power forecasting from 21st to 24th April 2016 [30]. The efficiency factor of each gas-fired unit is assumed to be 0.004 MW/m^3. The parameters for generating units are listed in Table 1.

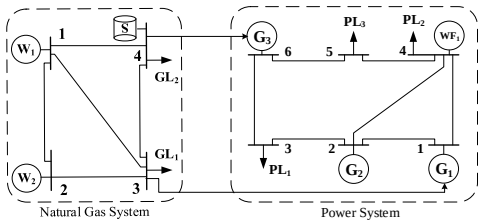

Fig. 2: Topology of a 4-node natural gas grid with a 6-bus power grid.

The time window includes 48 time intervals, and each time interval covers two hours. The lines 3-6 and 1-4 in the power grid need to be under maintenance in the given time window, and the corresponding durations of maintenance activities are 24 and 22, respectively. The costs of maintenance activities are \$600 and \$500 per time interval. For the natural gas grid, maintenance on the pipeline 2-3 should be implemented with \$500 per time interval, and the duration of maintenance activity is 31.

Table 1 Parameters for Generators

	G_1	G_2	G_3
Lower Limits (MW)	100	80	150
Upper Limits (MW)	300	200	350
Ramping Rates (MW/h)	25	20	7.5
Fixed Cost (\$)	5000	5000	5000
Linear Cost (\$/MW)	1200	1200	1200
Restart Cost (\$)	4000	4000	4000
Minimum Up Periods	4	3	2
Minimum Down Periods	2	3	3

4.1.2 Influences of ϵ and α on maintenance scheduling: This section analyzes the influences of wind power on maintenance scheduling for the integrated natural gas and power grid. Different percentages of wind power utilization are investigated. Table 2 shows the maintenance strategies with different wind power utilization, i.e., different values of ϵ and α. When we have $\epsilon = 0.3$ and $\alpha = 0.7$, maintenance on line $1-4$, line $3-6$, and pipeline $2-3$ should be performed from the periods 25 to 46, 25 to 48, and 7 to 37, respectively. When we have $\epsilon = 0.1$ and $\alpha = 0.9$, maintenance on line $1-4$, line $3-6$, and pipeline $2-3$ should be performed from the periods 25 to 46, 25 to 48, and 2 to 32, respectively. It is observed that the maintenance on natural gas grid has a marked difference. When we have a smaller ϵ and a larger α, there will be more wind power utilized in the power system, and in this case power generation from the units G_1, G_2, and G_3 will decrease. Because G_1 and G_3 are gas-fired units, power generation reduction from them leads to the reduction of natural gas consumption of the gas-fired units, and in consequence has an impact on maintenance on the natural gas grid.

Table 2 Maintenance Scheduling with different parameters

Parameters	Maintenance Scheduling
$\epsilon = 0.3, \alpha = 0.7$	L_{14}:25 $-$ 46, L_{36}:25 $-$ 48, PL_{23}:7 $-$ 37
$\epsilon = 0.1, \alpha = 0.9$	L_{14}:27 $-$ 48, L_{36}:25 $-$ 48, PL_{23}:2 $-$ 32

Fig. 3 shows the objectives when we have different percentages of wind power utilization, i,e., different values of ϵ and α. It is observed that a larger ϵ and a smaller α (i.e., a lower percentage of wind power utilization) lead to a larger objective. From the perspective of the mathematical model, a larger ϵ and a smaller α result in a relaxed feasible region due to the constraints (46) and (48). Because the optimization is to maximize the objective, a relaxed feasible region will result in an optimal solution with a larger objective. From the physical perspective, two reasons may lead to the larger objective. One is that a lower percentage of wind power utilization requires more power generation from units and in consequence leads to a higher revenue from these units. The other is that loss of load may be reduced when having less uncertainties due to less wind power when performing maintenance.

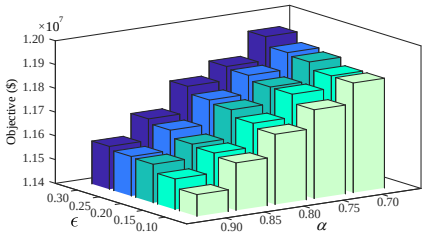

Fig. 3: Objectives with different values of ϵ and α.

4.1.3 Influences of Scenario Number on Maintenance scheduling: Because the revised sample average approximation method is used to deal with wind power uncertainty, the number of wind power scenarios impacts the maintenance scheduling. This section shows the influences of wind power scenarios on maintenance scheduling. Fig. 4 shows the optimization objectives with different wind power scenarios when having different values of the parameter α. For each value of the parameter α, the objective decreases and goes to a constant value. This constant value can be obtained with enough wind power scenarios. This indicates that more wind power scenarios result in a more accurate solution. From the perspective of the mathematical model, more wind power scenarios result in more constraints due to (46) and (47), i.e., a tight feasible region, and in consequence lead to a smaller objective since the optimization model is to find a maximum objective.

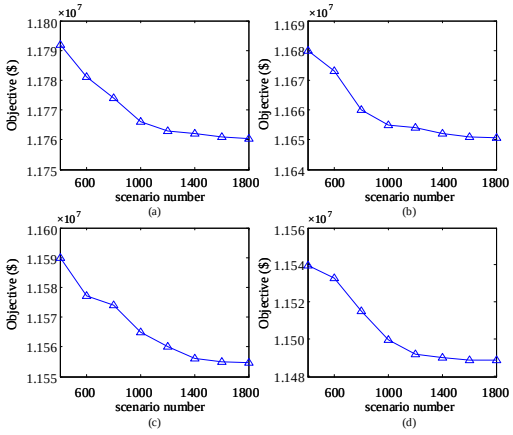

Fig. 4: Objectives with different wind power scenarios.
(a) Percent of wind power utilized $\alpha = 0.75$
(b) Percent of wind power utilized $\alpha = 0.80$
(c) Percent of wind power utilized $\alpha = 0.85$
(d) Percent of wind power utilized $\alpha = 0.90$

Table 3 shows maintenance strategies with different wind power scenarios. It is observed that we have the same maintenance strategies when having more wind power scenarios. This also shows that more scenarios of wind power leads to a more accurate solution. However, more scenarios cause computational intractability. The computation times for 200, 400, 600, 800, 1000, and 1500 scenarios are 225s, 698s, 1217s, 2151s, 3117s, 6172s, respectively. Because maintenance activities are defined as binary variables in the mathematical model, appropriate wind power scenarios can guarantee that the maintenance scheduling is optimal. For example, 600 scenarios in this case study have the same optimal maintenance scheduling as 1500 scenarios.

Table 3 Maintenance Scheduling with different scenarios

Scenario Number	Maintenance Scheduling
200	L_{14}:25 − 46, L_{36}:25 − 48, PL_{23}:12 − 42
400	L_{14}:27 − 48, L_{36}:25 − 48, PL_{23}:2 − 32
600	L_{14}:27 − 48, L_{36}:25 − 48, PL_{23}:4 − 34
800	L_{14}:27 − 48, L_{36}:25 − 48, PL_{23}:4 − 34
1000	L_{14}:27 − 48, L_{36}:25 − 48, PL_{23}:4 − 34
1500	L_{14}:27 − 48, L_{36}:25 − 48, PL_{23}:4 − 34

4.1.4 Influences of natural gas system on power system: Because natural gas to gas-fired units are limited by the natural gas grid, maintenance on pipelines directly impacts maintenance on the power system. Fig. 5 shows the loss of load in the power system when having different pipeline maintenance durations. It is observed that the loss of load is about 50MW when the pipeline maintenance duration is from 21 to 24 time intervals. This indicates that maintenance on pipeline P_{23} does not impacts gas supply to gas-fired units in the power system. However, when the pipeline maintenance duration is longer than 24 time intervals, the loss of load in the power system increases gradually. This means that maintenance over 24 time intervals or more will impact gas supply to gas-fired units in the power system and in consequence will lead to more loss of loads.

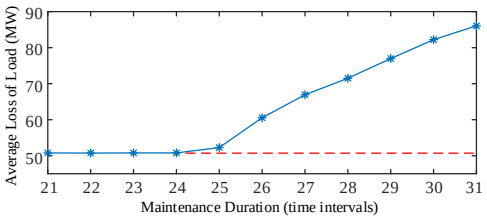

Fig. 5: Loss of load under different maintenance durations

4.2 20-node gas grid with 118-bus power grid

4.2.1 Data description: The data of the natural gas grid and the power grid can be found in [31] and [32], respectively. Wind power trends are the same as the trends in the first case, and the buses 2, 3, 5, 13, 14, 16, 44, 50, 52, 53, 82, 83, 84, 85, and 86 are connected to wind farms. The detailed data for wind power refer to [33]. The topology of the integrated system is shown as Fig. 6. Seven transmission lines 69-47, 69-70, 69-75, 69-77, 69-68, 49-69, and 49-47 need to be under maintenance within the given time window, and the durations of maintenance are 15 time intervals. Two pipelines 10-14 and 10-11 need to be under maintenance, and the durations of maintenance are 18 time intervals. The maximum numbers of pipelines and lines that can be under maintenance in one time interval are 1 and 2, respectively.

4.2.2 Influences of wind power on system maintenance: We first analyze the influences of wind power utilization on maintenance scheduling. Table 4 shows the objectives with different values of ϵ and α. A smaller ϵ and a larger α indicate more wind power utilized in power system. In this case power generation from generating units decreases, and in consequence the objective decreases accordingly.

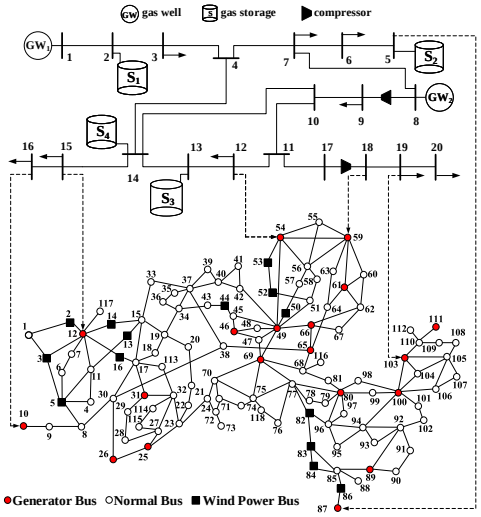

Fig. 6: Topology of the integrated system

Table 4 Objective Values ($\$10^9$) with Different Values of ϵ and α

	$\alpha = 0.7$	$\alpha = 0.8$	$\alpha = 0.9$
$\epsilon = 0.1$	3.109	3.096	3.085
$\epsilon = 0.2$	3.125	3.101	3.091
$\epsilon = 0.3$	3.131	3.104	3.095

We also analyze the influences of the number of wind power generators and wind pwoer forecast errors. Fig. 7 shows the objective values with different wind power generators and wind power forecast errors. Table 5 show the locations of different wind generators in different cases. It is observed that smaller wind power forecast errors and less wind power generators result in a larger objective, i.e., a more revenue. There are two reasons for this: 1) more power generation from generating units is required when having less wind power generators; 2) less loss of load occurs when having smaller wind power forecast errors. From the perspective of the mathematical model, a smaller wind power forecast error results in a smaller range for $\tilde{P}_{w,t,s}$, and in consequence results in a relaxed feasible solution region according to the constraints (46) and (47).

Table 5 Locations of wind generators in different cases

Number	Locations (Buses)
3	2, 3, 5
6	2, 3, 5, 13, 14, 16
9	2, 3, 5, 13, 14, 16, 44, 50, 52
12	2, 3, 5, 13, 14, 16, 44, 50, 52, 53, 82, 83
15	2, 3, 5, 13, 14, 16, 44, 50, 52, 53, 82, 83, 84, 85, 86

4.2.3 Influences of natural gas system on system maintenance: This section analyzes the influences of the natural gas system on system maintenance. Fig. 8 (a) shows the average loss of load for each time period when considering the influences of the natural gas grid, e.g., natural gas transmission capacity. Fig. 8 (b)

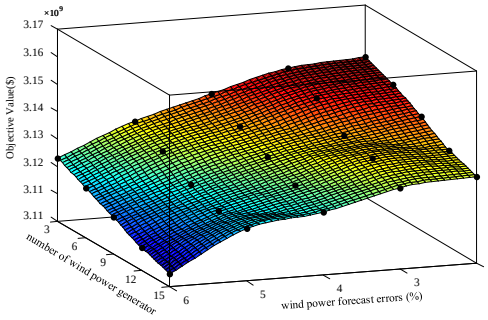

Fig. 7: Objectives with different wind power generators and wind pwoer forecast errors

shows the average loss of load for each time period when the influences of the natural gas grid are not included, i.e., the natural gas to the gas-fired units is not limited by the natural gas grid. It is observed that the first case in Fig. 8 (a) has larger loss of load compared to the second case in Fig. 8 (b) when having the same power forecast error. The main reason for more loss of load in the first case is the limited natural gas to the power grid due to the constraints of the natural gas grid. Therefore, the influences of natural gas systems on system maintenance should be included in practice.

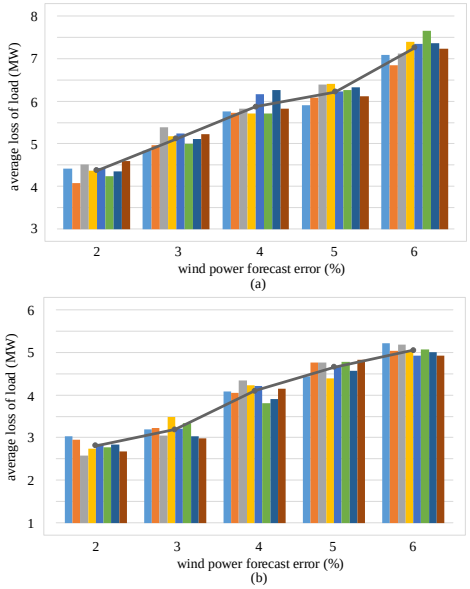

Fig. 8: Objectives with different wind power generators and wind pwoer forecast errors

4.2.4 Influences of piecewise linear approximation: Because the piecewise functions are used when modeling gas flow in pipelines, we also analyze the impacts of the number of piecewise functions on maintenance scheduling. Table 6 shows the objectives with different numbers of piecewise functions. It is observed that more piecewise functions lead to a smaller objective. From the perspective of mathematical model, more piecewise functions result in

a tighter feasible solution region according to the constraints (33)-(43). Because the optimization is to find a maximum objective value, a tighter feasible solution region leads to a smaller objective. More piecewise functions result in a more accurate solution, but also lead to a longer computation time. Take $\epsilon = 0.3, \alpha = 0.7$ as an example, the computation times are 3.6(h) and 8.1(h) when having 3 and 9 piecewise functions, respectively. Because maintenance scheduling is made off-line, a long computation time is acceptable in practice.

Table 6 Objective Values ($\$10^9$) with Different Piecewise Lines

	$k = 3$	$k = 5$	$k = 7$	$k = 9$
$\epsilon = 0.3, \alpha = 0.7$	3.149	3.138	3.131	3.127
$\epsilon = 0.1, \alpha = 0.7$	3.127	3.115	3.109	3.104

5 Conclusions

This paper presents a chance-constrained maintenance scheduling model for interdependent natural gas systems and power systems with wind energy integration. Chance constraints are used to model uncertainties of wind power, and these chance constraints are transformed into equivalent deterministic constraints by means of extended star-inequalities based on the sample average approximation. A piecewise linear approximation method is employed to convert the non-convex models of natural gas systems into a group of piecewise linear models, and the big-M formulation is employed to construct inequalities constraints for pipelines/lines that need to be under maintenance. Several tests on a 4-node natural gas gird with a 6-bus power grid and a 20-node natural gas grid with a modified IEEE 118-bus power grid demonstrate the effectiveness of the proposed model. The major findings are listed as follows. 1) A lower percentage of wind power utilization during the maintenance process can reduce the potential loss of load, and accurate wind power forecasting improves the system revenue during the maintenance window. 2) Shorter maintenance durations for power systems and natural gas grids can increase the system revenue during the maintenance window, especially when including the interactions between interdependent power systems and natural gas systems.

At present, a piecewise linear approximation approach is employed to transform the nonconvex and nonlinear Weymouth gas flow equations into a series of piecewise linear functions, which cause a gap to the original model. In the future work, some state-of-the-art methods based on second order conic relaxation can be used to improve the accuracy. In addition, second-order cone program (SOCP) formulations for describing AC power flow can replace DC power flow to improve the accuracy.

6 Acknowledgments

This work was supported by the Fundamental Research Funds for the Central Universities (2018B05514).

7 References

1 'Short-Term Energy Outlook', https://www.eia.gov/forecasts/steo/pdf/steo_full.pdf
2 'Annual Energy Outlook 2016 with projections to 2040', https://www.eia.gov/forecasts/aeo/pdf/0383(2016).pdf
3 '2002 system disturbances', https://www.eia.gov/outlooks/aeo/pdf/0383(2016).pdf
4 'Reliability Assessment Guidebook', http://www.nerc.com/files/Reliability%20Assessment%20Guidebook%203%201%20Final.pdf
5 'Global Wind Report 2016 - Annual Market Update', http://gwec.net/publications/global-wind-report-2/global-wind-report-2016/
6 'Annual Energy Outlook 2016 with projections to 2040', https://www.nrel.gov/docs/fy08osti/41869.pdf
7 'Global Wind Report Annual Market Update 2013', https://www.gwec.net/wp-content/uploads/2014/04/GWEC-Global-Wind-Report_9-April-2014.pdf
8 Zhao, B., Conejo, A., Sioshansi, R.: 'Coordinated Expansion Planning of Natural Gas and Electric Power Systems', *IEEE Trans. Power Syst.*, 2018, **33**, (3), pp. 3064-3075
9 Shao, C., Shahidehpour, M., Wang, X. F., Wang, X. L.: 'Integrated Planning of Electricity and Natural Gas Transportation Systems for Enhancing the Power Grid Resilience', *IEEE Trans. Power Syst.*, 2017, **32**, (6), pp. 4418 - 4429
10 Salimi, M., Ghasemi, H., et al.: 'Optimal planning of energy hubs in interconnected energy systems: a case study for natural gas and electricity', *IET Gener. Transm. Distrib.*, 2015, **9**, (8), pp. 695 - 707
11 Zlotnik, A., Roald, L., et al.: 'Coordinated Scheduling for Interdependent Electric Power and Natural Gas Infrastructures', *IEEE Trans. Power Syst.*, 2017, **32**, (1), pp. 600 - 610
12 He, Y., Yan, M., et al.: 'Decentralized Optimization of Multi-Area Electricity-Natural Gas Flows Based on Cone Reformulation', *IEEE Trans. Power Syst.*, 2018, **33**, (4), pp. 4531 - 4542
13 Yang, J., Zhang, N., et al.: 'Effect of Natural Gas Flow Dynamics in Robust Generation Scheduling Under Wind Uncertainty', *IEEE Trans. Power Syst.*, 2018, **33**, (2), pp. 2087 - 2097
14 Khani, H., El-Taweel, N., et al.: 'Real-time optimal management of reverse power flow in integrated power and gas distribution grids under large renewable power penetration', *IET Gener. Transm. Distrib.*, 2018, **12**, (10), pp. 2325 - 2331
15 Clegg, S., Mancarella, P., et al.: 'Storing renewables in the gas network: modelling of power-to-gas seasonal storage flexibility in low-carbon power systems', *IET Gener. Transm. Distrib.*, 2016, **10**, (3), pp. 566-575
16 Wang, C., Wei W., et al.: 'Strategic Offering and Equilibrium in Coupled Gas and Electricity Markets', *IEEE Trans. Power Syst.*, 2018, **33**, (1), pp. 209-306
17 Zhao, B., Conejo, A., et al.: 'Unit Commitment Under Gas-Supply Uncertainty and Gas-Price Variability', *IEEE Trans. Power Syst.*, 2018, **32**, (3), pp. 2394 - 2405
18 He, C., Wu, L., et al.: 'Robust Co-Optimization Planning of Interdependent Electricity and Natural Gas Systems With a Joint N-1 and Probabilistic Reliability Criterion', *IEEE Trans. Power Syst.*, 2018, **33**, (2), pp. 2140 - 2154
19 Shao, C., Shahidehpour, M., et al.: 'Integrated Planning of Electricity and Natural Gas Transportation Systems for Enhancing the Power Grid Resilience', *IEEE Trans. Power Syst.*, 2017, **32**, (6), pp. 2140 - 2154
20 Jalving, J., Abhyankar, S., et al.: 'A graph-based computational framework for simulation and optimisation of coupled infrastructure networks', *IET Gener. Transm. Distrib.*, 2017, **11**, (12), pp. 3163-3176
21 Ben-Tal, A., El Ghaoui, L., et al.: 'Robust Optimization' (Princeton, NJ: Princeton Univ., 2009)
22 Hojjat, M., Javidi, M.: 'Chance-constrained programming approach to stochastic congestion management considering system uncertainties', *IET Gener. Transm. Distrib.*, 2016, **10**, (3), pp. 566-575
23 Odetayo, B., Kazemi, M., et al.: 'A Chance Constrained Programming Approach to the Integrated Planning of Electric Power Generation, Natural Gas Network and Storage', *IEEE Trans. Power Syst.*, 2018, **33**, (6), pp. 6883-6893
24 Li, Y., Wang, J., et al.: 'Clustering-based chance-constrained transmission expansion planning using an improved benders decomposition algorithm', *IET Gener. Transm. Distrib.*, 2018, **12**, (4), pp. 935-946
25 Lubin, M., Dvorkin , Y.: 'A Robust Approach to Chance Constrained Optimal Power Flow With Renewable Generation', *IEEE Trans. Power Syst.*, 2016, **31**, (5), pp. 3840-3849
26 Zare, A., Chung , C.: 'A Distributionally Robust Chance-Constrained MILP Model for Multistage Distribution System Planning With Uncertain Renewables and Loads', *IEEE Trans. Power Syst.*, 2018, **33**, (5), pp. 5248-5262
27 Luedtke, J., Ahmed, S., Nemhauser, G.,: 'An integer programming approach for linear programs with probabilistic constraints', *Mathematical Programming*, 2010, **122**, (2), pp. 247-272
28 Correa-Posada, C. M., Sanchez-Martin, P.,: 'Security-Constrained Optimal Power and Natural-Gas Flow', *IEEE Trans. Power Syst.*, 2014, **29**, (4), pp. 1780-1787
29 Wang, Q., Guan, Y., Wang, J.,: 'A Chance-Constrained Two-Stage Stochastic Program for Unit Commitment With Uncertain Wind Power Output', *IEEE Trans. Power Syst.*, 2012, **27**, (1), pp. 206-215
30 'Wind Power Data', http://www.elia.be/en/grid-data/power-generation/wind-power
31 De Wolf, D., Smeers, Y.,: 'The gas transmission problem solved by an extension of the simplex algorithm', *Management Science*, 2000, **46**, (11), pp. 1454-1465
32 'IEEE 118-bus system data', http://motor.ece.iit.edu/DC/VSC/IEEE118.xls
33 Usaola, J.,: 'Probabilistic load flow with correlated wind power injections', *Electric Power Systems Research*, 2010, **80**, (5), pp. 528 - 536